Contrasted innate responses to two viruses in zebrafish: insights into the ancestral repertoire of vertebrate IFN-stimulated genes

Briolat, V.; Jouneau, L.; Carvalho, R.; Palha, N.; Langevin, C.; Herbomel, P.; ... ; Boudinot, P.

The Journal of Immunology

RESEARCH ARTICLE | MAY 01 2014

Contrasted Innate Responses to Two Viruses in Zebrafish: Insights into the Ancestral Repertoire of Vertebrate IFN-Stimulated Genes

Valérie Briolat; ... et. al

J Immunol (2014) 192 (9): 4328–4341.
https://doi.org/10.4049/jimmunol.1302611

Contrasted Innate Responses to Two Viruses in Zebrafish: Insights into the Ancestral Repertoire of Vertebrate IFN-Stimulated Genes

Valérie Briolat,*,† Luc Jouneau,‡ Ralph Carvalho,§,1 Nuno Palha,*,†,¶ Christelle Langevin,‡ Philippe Herbomel,*,† Olivier Schwartz,‖,# Herman P. Spaink,** Jean-Pierre Levraud,*,†,2 and Pierre Boudinot‡,2

Ease of imaging and abundance of genetic tools make the zebrafish an attractive model host to understand host–pathogen interactions. However, basic knowledge regarding the identity of genes involved in antiviral immune responses is still lagging in this species. We conducted a microarray analysis of the larval zebrafish response to two models of RNA virus infections with very different outcomes. Chikungunya virus (CHIKV) induces a rapid and protective IFN response. Infection with infectious hematopoietic necrosis virus is lethal and is associated with a delayed and inefficient IFN response. A typical signature of IFN-stimulated genes (ISGs) was observed with both viruses, but was stronger for CHIKV. We further compared the zebrafish and human ISG repertoires and made a genomic and phylogenic characterization of the main gene families. We describe a core set of well-induced ISGs conserved across vertebrates, as well as multigenic families diversified independently in each taxon. The conservation of ISGs involved in antiviral signaling indicates conservation of the main feedback loops in these pathways. Whole-mount in situ hybridization of selected transcripts in infected larvae revealed a typical pattern of expression for ISGs in the liver, gut, and blood vessels with both viruses. We further show that some inflammatory genes were additionally induced through IFN-independent pathways by infectious hematopoietic necrosis virus and not by CHIKV. This study provides a useful reference set for the analysis of host–virus interactions in zebrafish and highlights the differences between protective and non-protective antiviral innate responses. ***The Journal of Immunology*****, 2014, 192: 4328–4341.**

Viruses are ubiquitous pathogens, and all living organisms possess antiviral defenses. The evolution of these mechanisms, mirroring that of viral strategies, is fast and complex. Among metazoans, invertebrates appear to rely mainly on RNA interference–based mechanisms. In contrast, the innate antiviral defenses of vertebrates seem largely mediated by proteins, the expression of which is orchestrated by a group of cytokines known as IFNs. In mammals, type I IFNs directly induce the expression of a few hundred genes collectively known as IFN-stimulated genes (ISGs) (1, 2). ISGs encode a variety of proteins with diverse biochemical properties and functions (3, 4). Some have been shown to exert a direct antiviral role (e.g., MX proteins, PKR, TRIM5), which may act at any stage of the viral cycle. Others contribute to antiviral signaling, generating positive (e.g., STAT1, IFN regulatory factor [IRF] 7, TRIM25) or negative (e.g., SOCS proteins) feedback loops. A few ISGs also attract or activate cells with specialized roles in antiviral defense (e.g., CXCL9–11). The function of most, however, remains elusive. Recent approaches based on loss- and gain-of-function screens, performed on immortalized cell lines, allowed rapid progress of this field (2, 5). Nevertheless, the use of model organisms will be critical to unravel the role of these proteins, especially as many ISGs may be predicted to exert complex activity involving cell–cell cooperation or regulatory functions that cannot be detected by in vitro screening approaches. The quick evolution of most of these genes may complicate the transposition from model species to humans. However, the patterns of evolution of ISG families also convey functional information, as they bear witness to the evolutionary pressures in the arms race between host and pathogens. For example, host factors that directly interact with viral proteins

*Macrophages et Développement de l'Immunité, Institut Pasteur, 75015 Paris, France; †Centre National de la Recherche Scientifique, Unité de Recherche Associée 2578, 75015 Paris, France; ‡Virologie et Immunologie Moléculaire, Institut National de la Recherche Agronomique, 78352 Jouy-en-Josas, France; §ZF-screens, 2333 CH Leiden, The Netherlands; ¶Université Pierre et Marie Curie, 75005 Paris, France; ‖Unité Virus et Immunité, Institut Pasteur, 75724 Paris, France; #Centre National de la Recherche Scientifique, Unité de Recherche Associée 3015, 75015 Paris, France; and **University of Leiden, 2311 EZ Leiden, The Netherlands

[1]Current address: Institute for Environmental Studies, Vrije University, Amsterdam, The Netherlands.

[2]P.B. and J.-P.L. contributed equally to this work.

Received for publication September 30, 2013. Accepted for publication February 13, 2014.

This work was supported by French Agence Nationale de la Recherche Grant ANR-10-MIDI-009 (ZebraFlam and CHIK-HOST-PATH2 programs), by Fundação para a Ciência e a Tecnologia Grant SFRH/BD/60678/2009 (to N.P.), and by institutional grants from the Institut Pasteur, Centre National de la Recherche Scientifique, and Institut National de la Recherche Agronomique.

The microarray design and dataset presented in this article have been submitted to the Gene Expression Omnibus database (http://www.ncbi.nlm.nih.gov/geo) under accession numbers GPL7735 and GSE47057.

Address correspondence and reprint requests to Dr. Pierre Boudinot or Dr. Jean-Pierre Levraud, Virologie et Immunologie Moléculaire, Institut National de la Recherche Agronomique, 78352 Jouy-en-Josas, France (P.B.) or Macrophages et Développement de l'Immunité, Institut Pasteur, 75015 Paris, France (J.-P.L.). E-mail addresses: pierre.boudinot@jouy.inra.fr (P.B.) or jean-pierre.levraud@pasteur.fr (J.-P.L.)

The online version of this article contains supplemental material.

Abbreviations used in this article: CHIKV, Chikungunya virus; dpf, days postfertilization; FC, fold change; hpi, hour(s) postinfection; IFITM, IFN-inducible transmembrane protein; IHNV, infectious hematopoietic necrosis virus; IPA, Ingenuity Pathway Analysis; IRF, IFN regulatory factor; ISG, IFN-stimulated gene; RLR, RIG-I–like receptor; WISH, whole-mount in situ hybridization.

www.jimmunol.org/cgi/doi/10.4049/jimmunol.1302611

may be predicted to evolve under positive selection, and much faster than others implicated in a cascade where they contact only other host proteins (6). Family expansions may also be expected to arise from such evolutionary pressures. Importantly, to draw functionally meaningful conclusions, it is necessary to determine whether *ISG* orthologs present in distant genomes are indeed IFN and/or virus-inducible in the corresponding species.

Several features of the zebrafish (*Danio rerio*) make this model attractive for functional characterization of ISGs. The relatively basal position of the tetrapod–teleost split in the vertebrate tree makes the phylogenetic comparisons highly relevant, and functional testing is facilitated by the optical and genetic tractability of the zebrafish larva. The zebrafish has therefore recently gained acceptance as an immunological model and has been used to study host–pathogen interactions in a variety of bacterial or viral infections (7–9). In recent studies, we have conducted detailed analyses of two experimental viral infections in zebrafish larvae. The fish novirhabdovirus infectious hematopoietic necrosis virus (IHNV), a negative strand RNA virus that belongs to the Rhabdoviridae family, is systematically lethal in 3–4 d after inoculation, and primarily targets vascular endothelial cells; the host's IFN response occurs too late to protect the larvae (10). In contrast, the human alphavirus Chikungunya virus (CHIKV), a positive strand RNA virus that belongs to the Togaviridae family, induces a powerful IFN response, which allows larvae to recover from the infection despite a strong early replication (11). A number of virus-induced genes have been identified in zebrafish in our and other's work, but mostly based on homology approaches; no systematic study has been published so far in this species. Although IHNV and CHIKV are not natural viruses of zebrafish, none of which has been characterized so far, the comparison of the highly contrasted host responses to these two pathogens should provide useful insight as to the prototypical antiviral response of zebrafish to viruses. In particular, because CHIKV induces a very strong host IFN response, we expect a rather complete set of ISGs to be induced during this infection; the functional relevance of this response is demonstrated by the fact that knocking down IFN receptors results in death of CHIKV-infected larvae (11). In contrast, the inefficient host response to IHNV may arise from a generally lower IFN response, or from a selective blockade of a subset of ISGs; comparing the two responses will allow us to test this hypothesis. A global analysis of the host response to both viruses would also reveal possible additional response pathways to these viruses, which may interfere or synergize with the IFN response.

Large-scale analyses of transcriptome response to viral infection have been carried out in a number of other fish species, including Atlantic salmon head kidney cell response to SAV-1 (12), Atlantic salmon heart response to piscine myocarditis virus (13), orange-spotted grouper spleen response to Singapore grouper iridovirus (14), response of the grouper kidney cell line infected by betanodavirus (15), and Atlantic cod brain response to nervous necrosis virus (16). These studies generally addressed the transcriptional response of a particular tissue after infection with a given virus, and resulted in overlapping but largely distinct sets of modulated genes. To target the largest number of ISGs, these analyses were often performed with lymphoid tissues (i.e., spleen or kidney), thus revealing transcriptome modifications, which reflect mixed innate and adaptive responses in complex cellular contexts. Additionally, other studies have compared different states of transcriptome modulation between different conditions: Purcell et al. (17) studied the impact of infection with high and low virulence IHNV on kidney cells, whereas Martin et al. (18) compared the response of the salmon macrophage-like cell line SHK-1 to IFN type I (aka IFN-φ) and type II in one of the first comprehensive microarray-based ISG screenings in fish (18).

To produce a comprehensive description of the genes modulated by the virus infection in the whole zebrafish larva, we chose to follow the modifications of the transcriptome of the whole larva, using the validated microarray platform available in this species (19). At the selected developmental stage (5 d postferilization [dpf]), cells of the adaptive immunity are still absent and cannot skew the general description of the response. We carried out a comparative transcriptome analysis of the two highly contrasted infection models, IHNV and CHIKV. We then analyzed the kinetics and spatial expression of a series of genes, identifying a conserved pattern of expression for ISGs at the scale of the whole organism. Finally, we performed a genome-wide analysis of *ISG*-containing gene families.

Materials and Methods

Ethics statement

All animal experiments described in the present study were conducted at the Institut Pasteur according to European Union guidelines for handling of laboratory animals (http://ec.europa.eu/environment/chemicals/lab_animals/home_en.htm) and were approved by the Direction Sanitaire et Vétérinaire de Paris under permit B-75-1061.

Zebrafish husbandry

Wild-type AB zebrafish, initially obtained from the Zebrafish International Resource Center (Eugene, OR), were raised according to standard procedures (20). Eggs obtained by natural spawning were bleached and raised at 28˚C in Volvic source water. When eggs were used for imaging purposes, 1-phenyl-2-thiourea (Sigma-Aldrich, 0.003% final) was added at 24 h postferilization to prevent melanin pigment formation. At 3 dpf, just before infections, larvae that had not hatched spontaneously were manually dechorionated.

Viruses and experimental infections

IHNV strain 25.70 and CHIKV strain 115 were produced as described previously (10, 11), and injections and handling of larvae were performed as described in Levraud et al. (20). Doses of ~100 PFU/50% tissue culture–infective dose were injected in a volume of 1 nl, either i.v. in the caudal vein or aorta, posterior to the urogenital opening, or in the center of the yolk syncytial cell. Control larvae were injected with PBS. Larvae were then incubated at 24˚C (for IHNV) or 28˚C (for CHIKV).

Microarrays design

The microarray slides were custom-designed by Agilent Technologies. They contained in total 43,371 probes (60-bp oligonucleotides). Of these probes, a total of 21,496 probes were identical to the probes present on the Agilent probe set that is commercially available (Agilent Technologies, catalog no. 013223_D). Most of the additional probes were designed using the eArray software from Agilent Technologies (http://earray.chem.agilent.com/earray). Settings used were based on the following settings: base composition methodology, best probe methodology, and design with 3′ bias. The Agilent *D. rerio* transcriptome was used as a reference. A small number of probes were manually designed based on knowledge of particular polymorphisms for genes encoding protein families such as 14-3-3 proteins, chitinase-like proteins, and TLRs to obtain gene-specific probes. The microarray design has been submitted to the Gene Expression Omnibus database (http://www.ncbi.nlm.nih.gov/geo) under accession no. GPL7735. The following procedure was followed to get an updated/refined annotation: 1) Ensembl biomart web interface (http://www.ensembl.org/biomart) was used to extract the relationship between oligonucleotide identifiers and genes defined in Zv9 assembly (Ensembl gene identifier; gene symbol information). The extraction was restricted to oligonucleotides spotted on either the "Agilent G2518A," "Spaink leiden 2," or "Spaink leiden 3" microarray platform. 2) Oligonucleotide sequences were mapped on cDNA sequences corresponding to these genes using the alignment software bowtie (21), allowing fewer than three mismatches. All alignments were taken into account (using bowtie options "-a –best"). 3) We built a "zebrafish transcriptome" reference database with *D. rerio* RefSeq sequences. Oligonucleotide

sequences were again mapped on this sequence database using bowtie alignment software as above. Finally, all relationships between oligonucleotide probes and Ensembl genes were gathered in a unique annotation file, aggregating results from BioMart extraction, mapping of probes on Ensembl transcripts, and mapping of probes against RefSeq sequences.

RNA isolation, labeling, and hybridization

RNA was isolated from pooled larvae using TRIzol (Invitrogen), following the manufacturer's protocol. The integrity of the RNA was confirmed by laboratory-on-chip analysis using the 2100 Bioanalyzer (Agilent Technologies), using only samples with an RNA integrity number of at least 8. Labeling and hybridization were performed as described in van Soest et al. (22).

Microarrays analysis

Statistical analysis was performed using R software (http://www.r-project.org/). For probes linked to the same Ensembl gene, the average of signals was considered. A lowess normalization was operated for each microarray using Limma R package. Limma functions were used to perform the differential expression analysis. Raw p values have been adjusted using the Benjamini–Hochberg procedure. The entire dataset is available at the National Center for Biotechnology Information Gene Expression Omnibus (http://www.ncbi.nlm.nih.gov/geo/info/linking.html; accession no. GSE47057).

cDNA synthesis and quantitative real-time PCR

cDNA was synthesized using Moloney murine leukemia virus reverse transcriptase (Promega) and dT17 primer. Real-time quantitative PCR was then performed using the SYBR Green system (Applied Biosystems) in triplicate wells on an ABI3700 system (Applied Biosystems). Amplification yield was assessed in a titration assay (23) and used to deduce relative transcript amounts. Absolute quantification was performed by comparing levels in a reference cDNA mix with purified DNA fragments containing the target sequence quantified by UV spectrophotometry; this reference cDNA was then systematically included in quantification assays along the tested samples. EF1a was used as a normalization housekeeping transcript. Quantitative PCR primer pairs are described in Table I.

Whole-mount in situ hybridization

Whole-mount in situ hybridization (WISH) has been performed as in Thisse and Thisse (25) (with a hybridization temperature of 65˚C). The mmp9 probe was transcribed using SP6 polymerase from the pTOPOmmp9 plasmid provided by H.E. Volkman. To generate the other antisense probes, we RT-PCR amplified cDNA from infected larvae using an antisense primer with a 5′ terminal T3 (except for *E1chikV*: T7) promoter sequence added, a standard sense primer. PCR products were purified with a QIAquick PCR purification kit (Qiagen) and the probe was transcribed in vitro with polymerase (Promega). Unincorporated nucleotides were removed by purification on NucAway spin columns (Ambion). Sequences of primers used to generate the probes are provided in Table I.

Morpholino knockdown experiments

Morpholino antisense oligonucleotides (Gene Tools) were injected at the one to two cells stage as described (20). *crfb1* splice morpholino (2 ng) was injected together with *crfb2* splice morpholino (2 ng), knocking down all type I IFN receptors (26). Control morphants were injected with 4 ng control morpholino, with no known target. Sequences of morpholinos are given in Table I.

Transcriptome data and phylogenetic analysis

Initial search for ISG orthologs was performed using the Ensembl database (release v72). Orthology relationships were analyzed by inspection of the phylogenetic trees provided in this database. For some families, family members were further investigated by performing tblasn searches on zebrafish genome assembly Zv9 and RefSeq sequences at the National Center for Biotechnology Information, and further phylogenetic analysis when necessary.

Phylogenetic analyses

The evolutionary history was inferred using the maximum likelihood method with the JTT matrix–based model, pairwise deletion, and default parameters of Mega5 (27). The bootstrap consensus trees computed from 1000 replicates are shown with branches to scale, and the percentage of trees in which the associated taxa clustered together in the bootstrap test are indicated close to the branches.

Results

Microarray analysis of the zebrafish larva response to IHNV and CHIKV

To compare responses to the highly IFN-inductive, nonlethal CHIKV and to the lethal fish rhabdovirus IHNV, we performed

Table I. Primers used in this study

Gene	Forward Primer (5′ to 3′)	Reverse Primer (5′ to 3′)	Reference
PCR primers			
ef1a	GCTGATCGTTGGAGTCAACA	ACAGACTTGACCTCAGTGGT	(10)
ifnφ1 (secreted)	TGAGAACTCAAATGTGGACCT	GTCCTCCACCTTTGACTTGT	(10)
ifnφ1 (intracellular)	ACGGCAGCCTGAAATACGTT	GTCCTCCACCTTTGACTTGT	
ifnφ3	GAGGATCAGGTTACTGGTGT	GTTCATGATGCATGTGCTGTA	(10)
N-IHNV	CACTGGACTCAGAGACATCA	CTGCAAGCTTGTTGTTGGGA	(10)
rsad2/viperin	GCTGAAAGAAGCAGGAATGG	AAACACTGGAAGACCTTCCAA	(10)
irf7	TCTGCATGCAGTTTCCCAGT	TGGTCCACTGTAGTGTGTGA	(11)
E1-CHIKV	AARTGYGCNGTNCAVTCNATG	CCNCCNGTDATYTTYTGNACCCA	(11)
trim25	GAGCGGCGCTTCAAACAAAA	ATCAATTGCCAGCATGGCCT	(24)
isg15	AACTCGGTGACGATGCAGC	TGGGCACGTTGAAGTACTGA	
isg12.2	CTCAGATGGCATTCACAGCT	TGCACCTGCGCTTTGAAGAA	
irf1b	CGGATGAAGAGTCTGTCTCA	TGCCGAGTGAGCTCTAAGAT	
c4b	CCGACTATGCATTTGAAGTC	ACTGCATGTTTCCACTTGAG	
epd	TGAAAGTGGTTTCCACAGGG	GAGTACACCCTCTTCGAAAT	
mmp9	AGCTAGCGGATGAGTATCTG	GTTCAAAATCCTGTATGTGAC	
fkbp5	AATGTGGGGAAAGGTCAGGT	TCCAAGTGCACGTGGACA	
Primers for antisense WISH probe production			
isg15	ATGCAGCTGACTGTAAAACTGC	AACATTAACCCTCACTAAAGGGAATTATCCTCCTCGTAGACGGAGAG	
E1-CHIKV	AARTGYGCNGTNCAYTCNATGAC	TACGTAATACGACTCACTATAGGGAGATATTCAGGGGTTATTCGGCC	
epd	TGCATACAGTCAAGCTGCTC	AACATTAACCCTCACTAAAGGGAAAGCCATTGTTGGCAGTTTG	
irf7	AGTAGCGGAACTTCGGGTCA	AACATTAACCCTCACTAAAGGGAATGAGATCTCTAGGTCGAGGT	
rsad2	GTGACATCAAACCAACTTGG	AACATTAACCCTCACTAAAGGGAAGCACCTATATCAGCTTATGG	
isg12.2	ATGGGTCTACTTACAGCCGC	AACATTAACCCTCACTAAAGGGAACTAAATAAGAGCAAACCACCC	
Morpholinos			
crfb1	CGCCAAGATCATACCTGTAAAGTAA (splice morpholino)		
crfb2	CTATGAATCCTCACCTAGGGTAAAC (splice morpholino)		
control	GAAAGCATGGCATCTGGATCATCGA		

Table II. Selection of up- and downregulated genes after CHIKV and /or INHV infection

Symbol	Description	Ensembl Gene ID	CHIKV FC and Adjusted *p* Value	IHNV FC and Adjusted *p* Value
Upregulated genes				
IFN response				
isg12-2	IFN-stimulated gene 12-2	ENSDARG00000039243	**143.9*** **	**6.7***
isg12-1	IFN-stimulated gene 12-1	ENSDARG00000017489	**83.0*** **	**4.8***
isg15	IFN-stimulated gene 15	ENSDARG00000086374	**40.2*** **	**5.4***
rsad2	Radical S-adenosyl methionine domain containing 2; viperin	ENSDARG00000004952	**9.8****	**3.8***
IFITd3	IFN-induced (tetratricopeptide)	ENSDARG00000071012	**5.3****	**2.7***
IFITc	IFN-induced (tetratricopeptide)	ENSDARG00000057173	**6.5***	1.6
dram1	Damage-regulated autophagy; vig6	ENSDARG00000045561	**5.0****	0.6*
ifi35	IFN-induced protein 35	ENSDARG00000075643	**3.6****	1.1
isg12-4	IFN-stimulated gene 12-4	ENSDARG00000078389	**7.3****	2.0
isg12-3	IFN-stimulated gene 12-3	ENSDARG00000074217	**13.7*****	1.6
3′UTR isg12-7	Similar to IFN-stimulated gene 12-7	A_15_P118496	**4.1****	1.9*
Ifi44l	IFN-induced protein 44-like	ENSDARG00000010729	**9.1****	1.7*
mxa	IFN-induced GTP-binding protein MxA	ENSDARG00000021688	**9.8****	2.1*
mxe	IFN-induced GTP-binding protein MxE	ENSDARG00000014427	**8.2****	**2.5***
Complement				
C4b	Complement component 4B	ENSDARG00000038424	**5.1*****	**3.0***
MMP and signaling				
mmp9	Matrix metalloproteinase 9	ENSDARG00000042816	**2.7***	**7.6****
CD9c	CD9	ENSDARG00000044990	**34.3*****	**4.0***
junBb	junB proto-oncogene	ENSDARG00000088371	1.7*	**3.2****
Unc93b1	Unc-93 homolog B1	ENSDARG00000069114	0.56*	**4.9***
Transcription factors				
irf1b	IFN regulatory factor 1 (annotated irf11)	ENSDARG00000032768	**7.1*****	1.8*
irf7	IFN regulatory factor 7	ENSDARG00000045661	**11.0*****	2.0*
Stat1b	STAT1b	ENSDARG00000076182	**5.9****	1.7
Socs1	Suppressor of cytokine signaling 1	ENSDARG00000038095	**3.6***	1.2
cebpb	CCAAT/enhancer binding protein	ENSDARG00000042725	1.3*	**5.9****
Oxidative response and mitochondria				
ndufv1	NADH deH ubiquinone flavoprotein 1	ENSDARG00000036438	**0.37*****	**4.4***
ndufv3	NADH deH ubiquinone flavoprotein 3	ENSDART00000113587	**0.38*****	**2.6***
etfa	Electron transfer flavoprotein α	ENSDARG00000043944	0.48***	**3.0***
mt-tRNA	tRNA on mitochondrial genome	ENSDARG00000083519	1.5**	**3.7****
mt-tRNA	tRNA on mitochondrial genome	ENSDARG00000082716	0.9	**3.3****
mt-atp8	ATP synthase protein 8	ENSDARG00000063910	0.6*	**4.2****
mt-co3	Cytochrome *c* oxidase subunit 3	ENSDARG00000063912	1.4*	**4.0****
mt-co1	Cytochrome *c* oxidase subunit 1	ENSDARG00000063905	1.6**	**3.2****
mt-cyb	Cytochrome *b*	ENSDARG00000063924	0.6**	**2.9****
Secreted factors and binding proteins				
lgals3bpb-l	Similar to galectin-3–binding protein	ENSDARG00000040528	**3.7****	0.8
lgals3bpb	Galectin 3–binding protein	ENSDART00000101829	**4.0****	0.68*
lgals9l2	Galectin 9–like protein	ENSDARG00000041060	**3.0****	1.3
lgals9l1	Galectin 9–like protein	ENSDARG00000025903	**2.7****	1.2
lect2l	Leukocyte cell–derived chemotaxin 2	ENSDARG00000033227	**3.4*****	1.1
CXCL-C1c	CXC chemokine	ENSDARG00000075045	**2.6****	1.3*
CXCL-C13b	CXC chemokine	ENSDARG00000074487	**3.1****	1.3*
CCL-C5a	CC chemokine	ENSDARG00000058389	**3.0****	1.4
MHC and proteasome				
b2m	β_2-microglobulin	ENSDARG00000053136	**7.7*****	1.1
Tpsn	Tapasin	ENSDARG00000079402	**3.4****	0.9
Tpsn	Tapasin	ENSDARG00000045011	**2.8****	1.04
psme2	Proteasome activator subunit 2	ENSDARG00000033144	**2.5****	1
psma6b	Proteasome subunit, α type, 6b	ENSDARG00000043899	**2.5****	1.4*
psmb10	Proteasome subunit, β type, 10	ENSDARG00000001656	**2.9****	1.1
psmb11	Proteasome β 11 subunit	ENSDARG00000031885	**3.8****	1
psmf1	Proteasome inhibitor subunit 1	ENSDARG00000022652	**3.0*****	0.9
Trim				
trim25	Tripartite motif-containing 25	ENSDARG00000015865	**3.1*****	1.1
ftr-like	finTRIM-related protein; ftr80	ENSDARG00000067661	**3.0****	1.1
Translation				
rpl23a	Ribosomal protein L23a	ENSDARG00000006316	0.9	**2.9****
rpl32	Ribosomal protein L32	ENSDARG00000054818	1.4**	**2.6****
rpl34	Ribosomal protein L34	ENSDARG00000029500	1.1	**2.5****
rpl35a	Ribosomal protein L35a	A_15_P115161	1.5*	**2.6****
rpl37	Ribosomal protein L37	LOLS06369	1.0	**2.9****
rpl39	Ribosomal protein L39	ENSDARG00000036316	1.0	**2.6***
rpl9	Rribosomal protein L9	ENSDARG00000037350	1.1	**2.6****
rps8	Ribosomal protein S8	ENSDARG00000055996	1.0	**2.8****
rps5	Ribosomal protein S5	ENSDARG00000079026	1.1	**2.5****
rps12	Ribosomal protein S12	ENSDARG00000036875	1.0	**3.8****

(*Table continues*)

Table II. (*Continued*)

Symbol	Description	Ensembl Gene ID	CHIKV FC and Adjusted *p* Value	IHNV FC and Adjusted *p* Value
rps15	3′UTR of ribosomal protein gene	A_15_P109626	**0.4*** **	**7.7***
rps24	Ribosomal protein S24 isoform (intron)	A_15_P120710	0.7*	**2.6****
rpsa	Ribosomal protein S40	ENSDARG00000019181	**2.6****	1.6*
elf1g	Elongation factor 1-g	A_15_P110585	**0.48****	**2.7****
sars	Seryl-tRNA synthetase	ENSDARG00000008237	0.7**	**5.1****
Enzymes				
mov10b.1	Putative helicase mov-10	ENSDARG00000061177	**6.6*** **	1.5
zgc:154040	Putative phospholipase A_2	ENSDARG00000071326	**11.4****	1.4
ctssb1	Cathepsin S.b.1	ENSDARG00000075176	**4.3****	**0.5***
gpx1b	Glutathione peroxidase 1b	ENSDARG00000006207	**3.6*** **	0.8
cmpk2	Thymidylate kinase LPS-inducible (tyki)	ENSDARG00000031359	**3.5****	1.7
rnasel3	RNase-like 3	ENSDARG00000036171	**3.3*** **	1.1
adam8a	Metalloproteinase domain 8a	ENSDARG00000001452	**2.6****	**0.5****
atp2a1	ATPase, Ca^{2+} transporting, fast twitch 1	ENSDARG00000020574	0.8*	**5.4****
tgm1	Transglutaminase 1	ENSDARG00000019024	1.0	**3.0****
nat8l	*N*-acetyltransferase 8-like (EC 2.3.1.-)	ENSDARG00000077256	**0.5*** **	**2.9***
pfkfb3	6-Phosphofructo-2-kinase	ENSDARG00000001953	1.2	**2.5***
Apolipoproteins				
apoC1l	Apolipoprotein C1–like	A_15_P115491	**0.2*** **	**8.0***
zgc:193613	Apolipoprotein like	ENSDARG00000015866	0.8	**3.6****
apoa1	Apolipoprotein A-I precursor	ENSDARG00000012076	**0.4****	**2.6****
Dowregulated genes				
IFN response				
prkrir	Protein kinase, IFN-inducible dsRNA-dependent inhibitor, repressor	ENSDARG00000042489	0.8**	**0.3****
bril	Bone-restricted IFITM-like protein (aka IFITM5)	ENSDARG00000091273	**0.3*** **	**0.4***
Oxydative and inflammatory response				
fkbp5	FK506 binding protein 5	ENSDARG00000028396	1.0	**0.06****
dhrs1	Dehydrogenase/reductase 1 (SDR family) member 1	ENSDARG00000054300	**0.3*** **	1.8
pla2g12b	Phospholipase A_2, group XIIB	ENSDARG00000015662	**0.3*** **	**2.4***
prss35	Protease, serine, 35	ENSDARG00000017213	**0.3*** **	1.1
dhrs1	Dehydrogenase/reductase 1	ENSDARG00000054300	**0.3*** **	1.8
zgc:64031	Abhydrolase domain–containing 14B	ENSDARG00000023880	**0.3***	1.6
ucmab	Unique cartilage matrix-associated protein	ENSDARG00000005485	**0.2*** **	**2.4**
cyp26b1	Cytochrome P450 26B1 (Cyp26B1)	ENSDARG00000077121	1.0	**0.3****
hamp2	Hepcidin-2 precursor	ENSDARG00000053227	1.9	**0.3***
Others				
epd	Ependymin precursor	ENSDARG00000014745	0.7	**0.26****
mcam	Melanoma cell adhesion molecule	ENSDARG00000005368	0.9	**0.27****
fbln5	Fibulin 5	ENSDARG00000039273	0.7**	**0.29****
vsg1	Vessel-specific 1	ENSDARG00000045003	1.7**	**0.17****
tppp3	Tubulin polymerization-promoting	ENSDARG00000030463	0.7*	**0.31****
acta2	Actin, α2	ENSDARG00000045180	0.9	**0.32****
pppde2a	PPPDE peptidase domain–containing 2a	ENSDARG00000033140	1.0	**0.32****
meox1	Mesenchyme homeobox 1	ENSDARG00000007891	0.8*	**0.32****
rcn3	Reticulocalbin 3, EF-hand calcium binding	ENSDARG00000037961	0.6**	**0.34***
mad2l1	MAD2 mitotic arrest deficient-like 1	ENSDARG00000004713	0.9*	**0.33****
zgc:113183	SWI/SNF-related containing DEAD/Hbox 1	ENSDARG00000014041	0.8	**0.33****
kctd12.2	Potassium channel tetramerization	ENSDARG00000053542	1.1	**0.34****
taf6	TAF6 RNA polymerase II, TATA box BP	ENSDARG00000029135	0.7*	**0.34****
il13ra2	IL-13R, α2	ENSDARG00000039436	0.8	**0.35***
col8a2	Collagen, type VIII, α2	ENSDARG00000060893	0.7*	**0.35***
slc25a27	Solute carrier family 25. member 27	ENSDARG00000042873	0.55***	**0.35****
gli2a	GLI-Krüppel family member GLI2a	ENSDARG00000025641	0.91	**0.36****
mthfd2	Methylenetetrahydrofolate dehydrogenase 2	ENSDARG00000026666	0.7**	**0.36****
cx23	Connexin 23	ENSDARG00000054150	0.75	**0.38***

FC < 0.5 and FC > 2 are in bold.
Adjusted *p* values: *$p < 0.01$–0.05, **p < 0.005–0.01; ***$p < 0.001$–0.005.

a transcriptome analysis of infected zebrafish larvae. Based on our previous data (10, 11), we chose 48 h postinfection (hpi) as the time point that would allow us to detect a well-developed response to both viruses at a comparable stage of development. At this stage, IHNV-infected larvae are not moribund yet, so that the transcriptome analysis should not mainly reflect the general distress leading to death.

These experiments required infecting a large number of larvae, which was performed by i.v. microinjections in our previous studies (10, 11). Because this is challenging and time-consuming, we tested alternative infection methods that would still lead to the expected outcome in a reproductive fashion. Immersion of 3 dpf larvae in water containing either virus did not yield infection. However, in the case of CHIKV, we knew that i.v. inoculation results in infection of the yolk syncytial cell along various other cell types (11). This prompted us to test direct injection of CHIKV in the yolk, which is easier and faster than i.v. injection. We observed that both routes of inoculation led to similar patterns, as shown in

Supplemental Fig. 1A. We also found that yolk injection of CHIKV resulted in only slightly lower levels of expression of the CHIKV E1 transcript compared with i.v. injection, and to a slightly lower, but still very strong, upregulation of *ifnφ1* transcripts, with similar kinetics (Supplemental Fig. 1B), Thus, we chose to perform yolk injections for the microarray experiments. In contrast, injection of IHNV in the yolk did not result in infection, and we had to perform i.v. injections.

For each virus, three independent experiments were performed, and RNAs were extracted from pools of 30–70 larvae. RNAs from infected and control uninfected larvae from the same batch were labeled and hybridized to custom Agilent 44K microarray chips enriched in probes for predicted immune genes (19), which covers approximately half the zebrafish genome. After setting an arbitrary cutoff "fold" value at 2.5 (induction) or 0.4 (repression), we identified 583 features whose target expression was modulated by one or both viruses. A selection of these genes (based on strength of modulation and on predicted functions) is shown on Table II. Genes upregulated by CHIKV were induced by IHNV at a lower level (Fig. 1A, black ellipse). This pattern is well consistent with an induction mediated by type I IFNs, because CHIKV induces a much stronger IFN response compared with IHNV. In contrast, most genes well induced by IHNV infection were not significantly modulated by CHIKV (Fig. 1A, gray ellipse), suggesting induction of distinct pathways. The correlation between the two responses was relatively poor, with only 15 genes significantly up regulated >2.5-fold (and none downregulated) by both viruses (Fig. 1B).

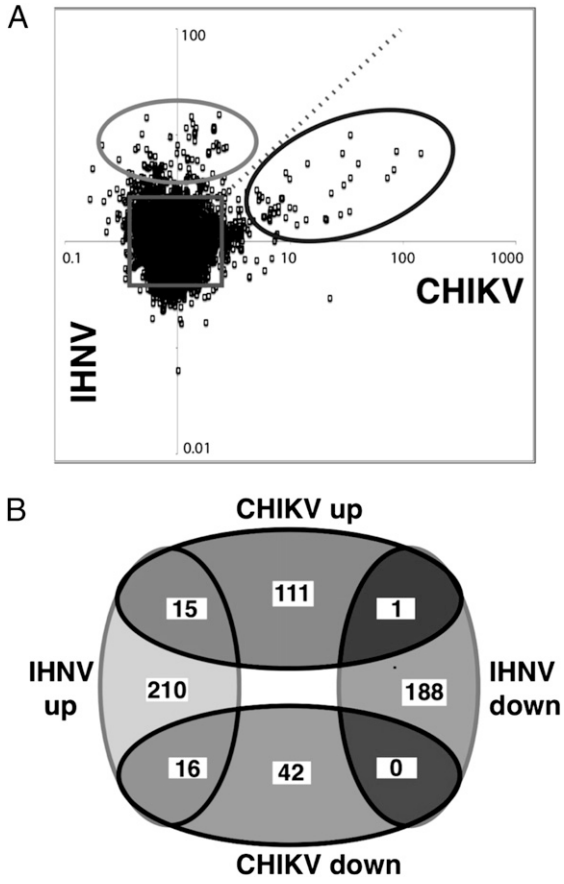

FIGURE 1. Global transcriptome response of zebrafish larvae to IHNV and CHIKV infection. (**A**) FC/FC representation. Multiple probes corresponding to unique genes were aggregated. The average value is represented for all genetic features addressed by the array. The black ellipse highlights the group of genes strongly upregulated by CHIKV and moderately by IHNV, as expected of ISGs. The gray ellipse highlights genes upregulated by IHNV only. The gray square indicates thresholds considered in the analysis (FC > 2.5 or FC < 0.4). (**B**) Venn diagram of genetic features providing differential signals (adjusted p value of <0.05; FC > 2.5 or FC < 0.4) between infected and control for IHNV and CHIKV.

Kinetics of gene induction

By performing quantitative RT-PCR on a subset of genes, we confirmed these findings and extended them to obtain a kinetic picture of the response (Fig. 2 and data not shown). Modulation of expression observed from microarray data was confirmed for this selection of genes, with the notable exception of two genes presumably downmodulated by CHIKV, *apoC1L* and *ucmab*. Both were represented by a single probe on the array in their predicted 3′ untranslated region, whereas our PCR primers targeted open reading frames, suggesting that for these genes, CHIKV infection may be associated with use of alternative polyA sites, but this matter was not investigated further. Kinetics of infection, measured by expression of viral genes (Fig. 2, *top panels*), were consistent with previously published studies (10, 11), with CHIKV reaching a peak at 24 hpi then slowly declining, whereas IHNV continuously increased until the death of the larvae. Interestingly, genes orthologous to well-known ISGs (*rsad2/viperin*, *isg12.2*, *isg15*, *trim25*, *irf7*, *irf1b*) all followed the same kinetics, even though some may be induced 100-fold more than others; these kinetics matched very well the kinetics of the induction of the secreted isoform of *ifnφ1*. The only exception was a decrease in *isg12.2* expression at the most advanced stage of IHNV infection. However, this was not observed in all experiments and is likely to be an artifact linked to the very low level of expression of this gene (see Fig. 2, *left center panel*). Lower fold changes (FCs) and different kinetics of induction upon CHIKV infection were observed for other inducible genes not expected to be ISGs such as *c4b* or *mmp9*, consistent with their induction by separate pathways (Fig. 2, *middle bottom panel*). The kinetics of gene induction by IHNV infection are more complex, but suggest that *mmp9* was upregulated early and did not show the delay observed for the IFN response (see Fig. 2, *right panel center* and *bottom*).

Spatial patterns of expression

We used WISH to determine the site of expression of some selected genes. This analysis was performed at the peak of the response for CHIKV (24 hpi), and at 48 hpi for IHNV, as responses were quite weak at 24 hpi, whereas infection-induced damage at 72 hpi caused larvae to fall apart during the hybridization process. Fig. 3 illustrates spatial expression pattern of different ISGs regarding virus tropism represented by localization patterns of CHIKV- or IHNV-infected cells (Fig. 3A). Consistently with quantitative RT-PCR results, which showed that the basal expression of strongly inducible ISGs such as *isg15* was quite low, very little signal was detected in control, uninfected larvae; however, a strong signal was detected after infection with CHIKV, and a weaker but visible signal was detected in IHNV-infected larvae (Fig. 3B). The strongest *isg15* signal was detected in the liver after both virus infections; specific signal was also detected in the gut and, for CHIKV-infected larvae only, in the vasculature. Remarkably, the other ISGs assessed, that is, *irf7, rsad2/viperin*, and *isg12.2*, had a globally similar pattern of expression (Fig. 3C). However, closer examination revealed some preferences, with *irf7* being expressed more strongly in vessels (and also visible in dispersed cells, probably leukocytes), whereas *rsad2* and *isg12.2* are only modestly expressed in the gut and liver, respectively.

We also tested *mmp9*, for which a different pattern might be expected to arise from a different stimulus, because it is not

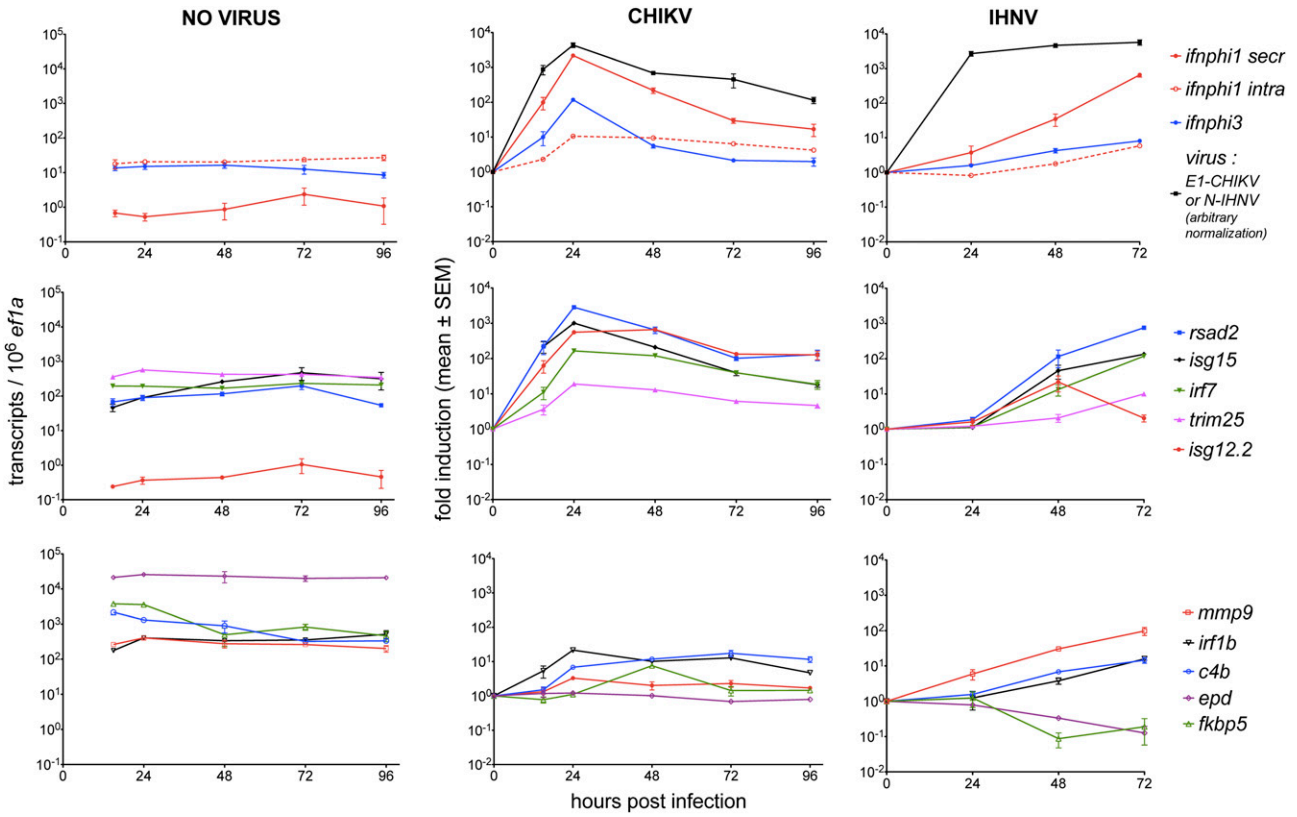

FIGURE 2. Kinetics of transcriptomic responses. Quantitative RT-PCR analysis; mean ± SEM from three pools of three to five larvae per point; one representative experiment out of two or more is shown. *Left panels* show basal expression in uninfected larvae raised at 28˚C; absolute quantifications were normalized to *ef1a* expression. *Center* and *right panels* display expression measured in CHIK- and IHNV-infected larvae, respectively (i.v. infections in both cases); in this case, results are reported as the ratio of expression in infected larvae to uninfected controls. The expression of viral genes (CHIKV-E1 or N-IHNV), which are not detectable in uninfected larva, is shown on the *top panels*. In this case, normalization was made by dividing the measured copy number arbitrarily by 1000 copies/10^6 ef1a copies.

a typical ISG. Indeed, the pattern of *mmp9* expression induced by IHNV was strikingly different from that of ISGs, with a staining of superficial cells, probably in the epidermis (Fig. 3D). Finally, we also tested a few downmodulated genes. Although no clear pattern of expression for *fkbp5* could be observed (not shown), a striking pattern was observed in uninfected larvae for the *epd* gene encoding ependymin (Fig. 3E), in agreement with the pattern available on the Zebrafish International Resource Center Web site (http://zfin.org/cgi-bin/webdriver?MIval=aa-fxfigureview.apg&OID=ZDB-FIG-070503-464) (28): a subset of cells in the head (and possibly in the endocrine pancreas) expresses *epd*. Despite the gene name, these cells do not line brain ventricles and are thus not ependymal; instead, they are located on the brain external surface, apparently ensheathing some blood vessels. IHNV infection induced a dramatic reduction in the number of *epd*-expressing cells, especially in the dorsal cranium. This, consistent with the infection patterns (see figure 2D of Ref. 10), suggests that *epd*-expressing cells are targeted and killed by the virus. Similarly, *vsg-1*, an endothelium-specific gene (29), is downmodulated by IHNV, and this expression was lost in many vessels in IHNV-infected larvae (not shown), in accordance with our previous finding that vascular endothelium is a primary target of IHNV (10).

Pathway analysis of the responses

IFN-related pathways. Analysis of the list of modulated genes by GenMAPP and Ingenuity Pathway Analysis (IPA) identified several biological pathways induced by the viral infections. IFN signaling was found enriched by IPA for both viruses, although with more genes involved and a lower *p* value for CHIKV; type I IFNs were predicted as main upstream regulators in both cases. Many genes previously characterized as ISGs or homologous to well-known human ISGs were found to be highly upregulated by CHIKV, and to a lesser extent also by IHNV (Fig. 4, Table II). Analysis of genes presumably involved in signaling pathways upstream of IFN induction was not as straightforward, probably reflecting that activation of these pathways involves posttranslational modifications more often than transcriptional modulation. The detection of viruses may happen either in the cytosolic compartment of cells via the RIG-I–like receptor (RLR) pathway, or in endosomal compartments via the TLR pathway. We have previously implicated the RLR pathway in the zebrafish response to CHIKV, because knockdown of MAVS/IPS-1, a central adaptor of this pathway, was found to strongly reduce IFN induction (11). No modulation of the *mavs* transcript was seen with either virus, which was consistent with previous observations (30, 31); this was also the case for most genes involved in the RLR pathway (Supplemental Fig. 2), with the notable exceptions of *trim25*, *isg15*, and *irf7*, all orthologs of known ISGs, involved in signaling feedback loops. A similar picture emerged from the analysis of the TLR pathway (Supplemental Fig. 2); neither virus modulated most genes in this pathway. A few genes induced by IHNV included proteins typically involved in responses to bacteria rather than to viruses (e.g., *mmp9*). Again, this suggests that in addition to the typical virus-induced IFN response, IHNV triggers other inflammatory pathways.

Conspicuously absent from the list of IHNV- or CHIKV-induced genes were the type I IFNs themselves, *ifnφ1–4*. The microarray did not include probes for *ifnφ3* and *ifnφ4*; *ifnφ4* does not appear to be involved in the antiviral response (32), and we

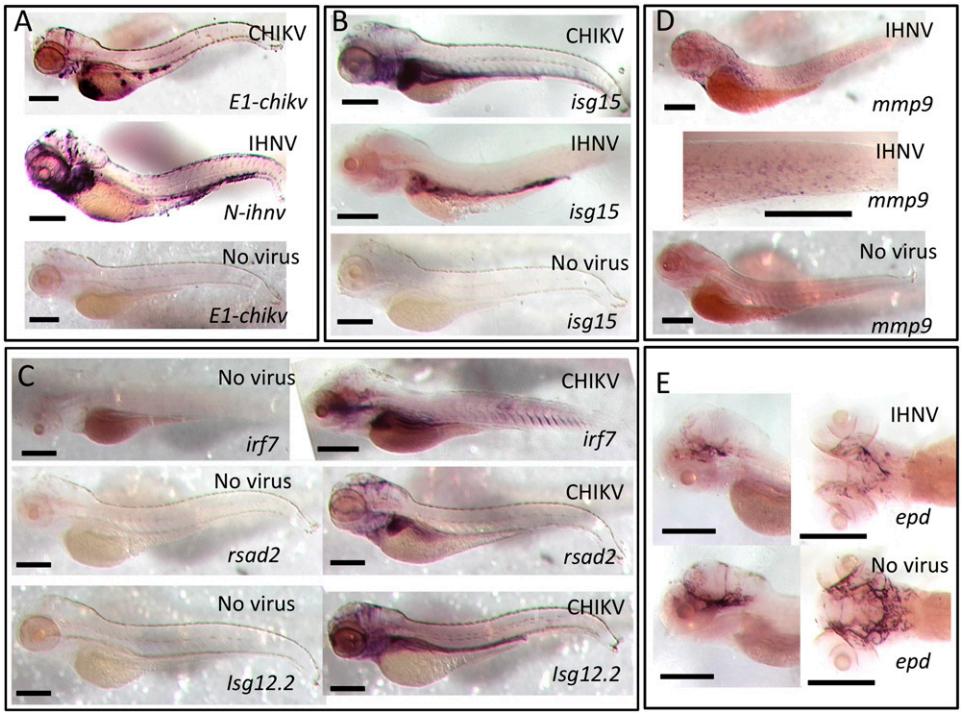

FIGURE 3. Spatial expression patterns. WISH. Probes are indicated in bottom right of each panel; infection type is indicated in top right corner. For CHIKV infections, analysis was performed at 24 hpi; for IHNV, at 48 hpi. (**A**) Viral genes, used as an example of the typical distribution of infected cells. The uninfected control for the *N-ihnv* probe is not shown, but no signal is visible (as previously shown in Ref. 10). (**B**) Expression of *isg15* chosen as a typical ISG more strongly induced by both viruses, but more strongly by CHIKV. Uninfected control is shown at 4 dpf (5 dpf controls do not show any signal either). (**C**) Expression of three other ISGs (*irf7*, *rsad2,* and *isg12.2)* in control (4 dpf) and CHIKV-infected larvae. (**D**) Expression of *mmp9*, a non-ISG induced more strongly by IHNV than CHIKV. *Middle panel*, Close-up of the tail region. Control shown at 5 dpf. (**E**) Expression of epd, a gene downregulated by IHNV. Head regions: lateral views on left, dorsal views on right. Uninfected control is shown at 5 dpf. Scale bars, 250 μm.

have found previously *ifnφ2* to be expressed by adult zebrafish, but not at the larval stage (26, 33). The apparent lack of induction of *ifnφ1* is explained by the existence of two alternative transcripts of this gene: a constitutively expressed transcript encoding a putatively nonfunctional protein lacking a signal peptide, and an inducible transcript encoding the active cytokine (32). Because the *ifnφ1*-specific probes on the microarray do not discriminate between the two forms, the induction of the active cytokine transcript has been likely masked by the constitutive expression of the alternative transcript; indeed, as can be seen in Fig. 2, the poorly inducible, nonsecreted isoform has an ~30-fold higher basal expression level than the secreted isoform.

Other pathways (e.g., redox, mmp, liver X receptor). Although typical inflammatory pathways such as "airway pathology and pulmonary diseases" or "granzyme A" were found by IPA from the CHIKV response in addition to IFN signaling, additional pathways were revealed as significantly enriched in the response to IHNV: 1) the EIF2 signaling pathway, which refers to the upregulation of a number of ribosomal protein genes (Supplemental Fig. 3), many of which were upregulated by IHNV infection. Although it is generally accepted that virus infection induces a shut-off of cell protein production, this pattern might either represent a compensatory transcriptional response or a virus-directed modification of cell syntheses beneficial to the pathogen production (34). 2) The pathway "mitochondrial dysfunction" was also pointed out after IHNV infection; this is due to the upregulation of eight genes encoded by the mitochondrial genome and/or involved in redox regulation, and to the strong downregulation of *fkbp5* in IHNV-infected larvae. Notably, two of them (*ndufva* and *etfa*) were downregulated in CHIKV-infected fish. 3) The liver X receptor/retinoid X receptor pathway was also highlighted after IHNV infection, comprising genes upregulated by both viruses such as complement genes or *mmp9*, but also the apolipoproteins, which were modulated by IHNV only, and phospholipase A_2, which was induced by IHNV and repressed by CHIKV. Finally, "liver necrosis, cell death and inflammation" was among the top "tox lists" of IPA for both viruses, which could be related to the strong cytopathic effect of these viruses, as well as to the spatial expression pattern of modulated genes (see above).

IFN signaling is involved in the upregulation of key virus-induced genes

Genes strongly induced by CHIKV, but less so by IHNV, are presumably induced by the strong and protective IFN response in CHIKV-infected fish; indeed, most of these genes are orthologous to well-known mammalian ISGs. To check the IFN dependency of the upregulation observed during the infection for a selection of genes, we knocked down the two zebrafish type I IFN receptors (26) using antisense morpholinos, infected larvae with CHIKV, and measured gene expression by quantitative RT-PCR at the peak of the response. When compared with control morphants (Fig. 5), induction of genes such as *rsad2/viperin*, *isg12.2*, *isg15*, *trim25*, and *irf7* was severely reduced, indicating that their induction was IFN-dependent, as expected. In contrast, *mmp9* and *irf1b* induction appeared to be IFN-independent. This was expected for *mmp9*, but is surprising for *irf1b*, the human ortholog of which is an ISG. Therefore, we should be aware that induction by CHIKV does not necessarily equate induction by type I IFN, even for ISG orthologs. Nevertheless, it does seem to be the case for most of the genes we tested, which prompted us to perform a genome-wide analysis of the orthologs of human ISGs.

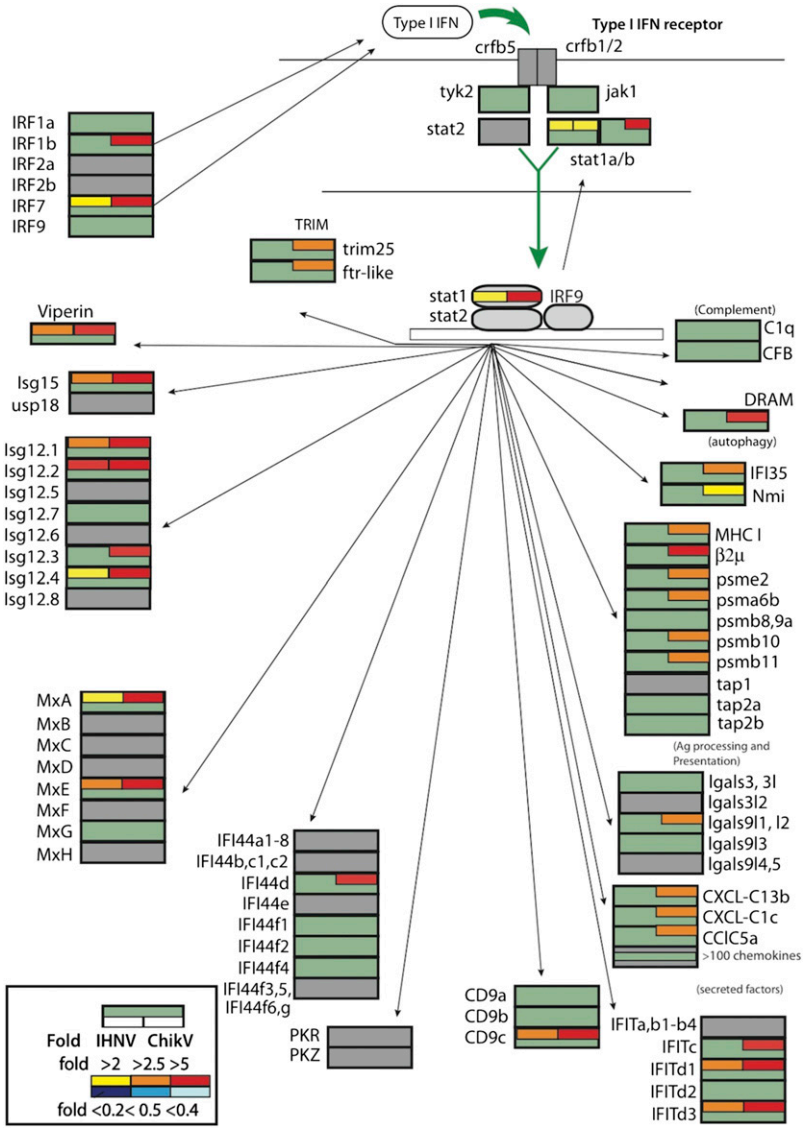

FIGURE 4. ISG pathway. Analysis of gene expression responses downstream of type I IFNs upon IHNV and CHIKV infection of the zebrafish larvae, according to the microarray data. The expression profiles at 48 hpi by IHNV or CHIKV (infected versus control) were simultaneously mapped on the IFN pathway. Gene boxes are color coded according to FC as indicated. Gray denotes genes that were not represented on the array. The pathway is based on knowledge of IFN signaling and ISG expression in mammalian species and is not meant to be exhaustive; most interactions remain to be experimentally confirmed in zebrafish. We attributed new names to many zebrafish genes that did not have explicit names; their exact identity can be found in Supplemental Table I.

Genomic and expression analysis of ISG orthologs

Are zebrafish genes orthologous to human ISGs generally IFN inducible? Although our initial GenMAPP and IPA analysis identified a number of genes as being induced downstream of type I IFNs (displayed in Fig. 4), there are many other, less well-known ISGs. We took advantage of the exhaustive human ISG list compiled by Schoggins et al. (2) based on a compilation of a dozen human microarray studies. We searched the zebrafish genome for the orthologs of these genes, with the help of the phylogeny tools at Ensembl.org (release 72); the results of this analysis are provided as a searchable Excel file with links to gene pages (Supplemental Table I). This table includes 445 human genes for which a total of 593 zebrafish orthologs were found, of which 280 were represented on the microarray.

As expected, we found within this dataset the genes highly induced by the viral infection. However, a significant enrichment was detected even among genes with modest levels of induction (Fig. 6). Also, the proportion of genes reproducibly modulated between replicates (corrected $p < 0.05$, regardless of the actual FC) was higher within ISG orthologs (146 of 280 genes) compared with the whole dataset (5,188 of 12,524) (χ^2 test, $p < 0.001$). Thus, in addition to the well-known, strongly induced ISGs, a large number of modestly inducible genes should also be included in the core vertebrate group of IFN (or rather, virus)-inducible genes. These observations led us to propose a tentative estimation of the size of the core set of ISGs conserved between zebrafish and humans; subtracting the global distribution of induction of CHIKV-induced genes to the distribution of induction of zebrafish orthologs of human ISGs, one obtains a rough assessment of 53 ISGs represented on the microarray (Fig. 6, highlighted area). Given that approximately half of genes are represented on the array, both for the entire dataset and for the ISG orthologs, the order of magnitude of the size of the core ISG subset shared by fishes and mammals would be 100 genes.

Analysis of ISG-containing multigene families

A large number of mammalian ISGs constitute multigene families; Table III shows that it is also the case in the zebrafish. Phylogenetic relationships between human ISGs and their zebrafish orthologs indicate that these genes are prone to extensive duplication in each evolutionary branch: 35 examples of "many-to-many" orthology relationships can be observed in Supplemental Table I, which are ~7-fold more frequent than for the overall genome comparison (233 such relationships in total) (35). Fami-

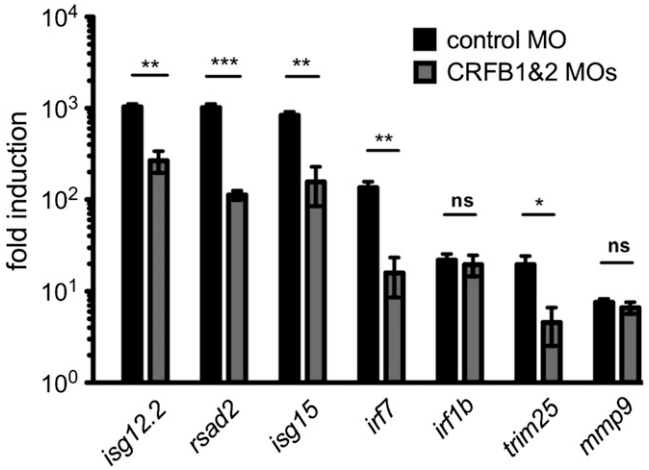

FIGURE 5. IFN dependence of response. Gene induction by CHIKV at the peak or response (24 hpi) after i.v. infection; FC compared with uninfected larvae. Quantitative RT-PCR; means ± SEM for three pools of five larvae; one representative experiment out of two. At the one cell stage, embryos had been injected with a control morpholino oligonucleotide (blue bars) or with a mixture of CRFB1- and CRFB2-specific antisense morpholinos (red bars) to knock down IFN receptor expression. Levels of FC compared by unpaired *t* test: $*p < 0.05$, $**p < 0.01$, $***p < 0.001$.

lies were generally more diversified in zebrafish than in humans, with the more extreme case being the IFI44 family with 20 zebrafish members versus 2 human members. However, a few diversified human ISG families have a single zebrafish ortholog (e.g., the apolipoprotein L and the metallothionein 1 families). Some prominent human ISG families are also totally absent from the zebrafish genome, including the APOBEC3, OAS, and AIM2/IFI16 families (Table III). Apparently, these three families are absent in all other teleosts as far as we can tell.

When we looked up these genes in our array dataset, we found that in a few families (e.g., the IFIT family) all tested members were induced by CHIKV infection, whereas many others (e.g., IFI44, ISG12 families) included both induced and noninduced genes. A similar situation is found in many human ISG-containing

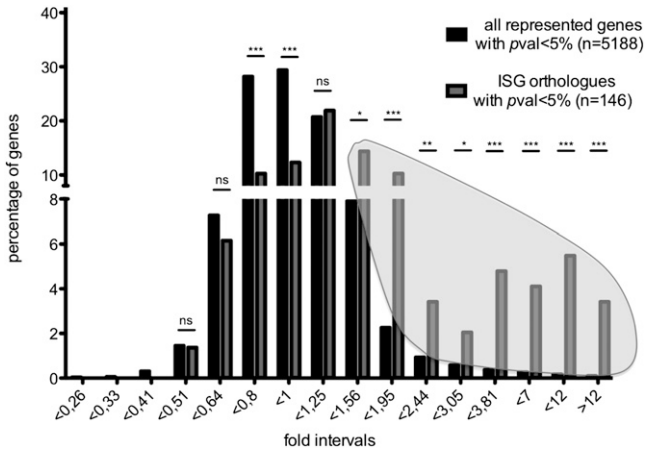

FIGURE 6. Distribution of CHIKV-inductions of ISG orthologs, compared with the overall dataset. Distribution of genes with an Ensembl ID on the microarray dataset, according to FC by CHIKV (when corrected *p* value of < 0.05). For clarity, only the upper limit of the considered interval is indicated under the horizontal axis. Comparisons of the entire set and of the subset of ISG orthologs are shown. The shaded area depicts our estimate of the number of specifically ISGs. Differences in frequencies of ISG orthologs versus other genes within a given interval were tested by a χ^2 test ($*p < 0.05$, $**p < 0.01$, $***p < 0.001$).

families, despite a misleading nomenclature (e.g., IFN-inducible transmembrane protein [IFITM] 5, aka *BRIL* for bone-related IFITM-like protein (36), got its current official name from its homology and synteny to *IFITM1–3*, but it is not an ISG).

Phylogenetic analysis (Fig. 7, Table III) separated the families into two main categories: "old" families, which diversified before the tetrapod/teleost split ~450 million years ago, resulting in the presence of one or two zebrafish orthologs for most human members of the family; and "young" families, where all human members on the one hand, and all zebrafish members on the other hand, appeared through recent, independent diversifications from a single gene present in the zebrafish/human common ancestor. Typical old families include IRF, SOCS, and STAT; typical young families include IFI44, IFIT, ISG12/IFI27, and MX. A few families were in an ambiguous position such as IFITM/CD225 and PARP.

We find in this study that there is a remarkable correspondence between ISG-containing families in zebrafish and humans. In old families, human ISGs are generally orthologous to zebrafish ISGs, and the same is true for non-ISGs members. Of course, such relationships cannot be established for young families. Interestingly, some young families (e.g., ISG12) contain both ISGs and non-ISGs in human and zebrafish.

Discussion

Rationale of the study

Innate immunity to viruses is orchestrated by type I IFNs. Several pathways downstream of viral pattern receptors, including TLRs and RLRs, lead to a sharp upregulation and secretion of type I IFNs. These highly inducible cytokines have specific receptors on most cell types that signal via JAK/STAT pathways and induce a large number of ISGs. This system is remarkably conserved across vertebrates, and fish as well as mammals possess typical type I IFNs and IFN receptors. However, the evolutionary pattern of the effectors (the ISGs) and their functions is much less clear. In fact, a direct activity against many viruses has been shown for only relatively few ISGs, and the functions and mechanisms of action of most ISGs remain elusive. Because their evolutionary history conveys information as to their function, and because in vivo functional testing of ISGs would be facilitated in a genetically tractable organism, we wanted to identify the conserved "core" set of virus-induced genes shared by humans and zebrafish. To do so, we analyzed the transcriptional response of the zebrafish larva to two RNA viruses, one known to induce a strong and protective IFN response (CHIKV) and another for which this response is delayed and nonprotective (IHNV). Although CHIKV and IHNV are not natural zebrafish viruses (none of which are known at the moment), they are used in this study as stimulators of antiviral pathways, in the same way that non-natural viruses or synthetic inducers such as polyinosinic-polycytidylic acid have been instrumental in identifying ISGs in mammals. We then compare the set of ISGs expressed in the zebrafish larva, which represents the most commonly used stage in this model for functional studies as well as for drug screening, to the complete repertoire of human ISGs (as described in Ref. 2) to determine functional and evolutionary patterns that will be relevant for further studies in the field.

The CHIKV-induced response is mainly IFN-dependent and defines a core set of highly induced ISGs conserved across vertebrates

Studies of the virus-induced transcriptional response in fish were performed in a variety of infectious systems, identifying genes induced in specific tissues. In our study, we measured the FC in the

Table III. ISG-containing families

Selected Families[a]	Human Members[b]	Zebrafish Members[b]
Tetrapod only		
AIM2/IFI16	***aim2; ifi16****; mnda; pyhin1*	—
APOBEC3	***apobec3a, b***, *c, d, f,* ***g,*** *h*	—
CLEC4	*clec4a, c,* ***d, e,*** *6a*	—
OAS	***oas1, 2, 3, l***	—
Teleosts and tetrapods independently diversified in teleosts and/or tetrapods (young)		
APOL	***apol1–3; apol6;*** *apol4–5*	*apol*
CLEC2	***cd69; clec2b;*** *clec2-a, -d, -l; klrg12*	*clec2*
GBP	***gbp1–5***, *gbp6–7*	***gbp-a1***, *-a2, -a3, -b, -c, -d, -e1, -e2*
IFI27/ISG12	***ifi6; ifi27;*** *ifi27l1; ifi27l2*	***Isg12-1, -2, -3, -4***, *-5, -6, -7, -8*
IFI44	***ifi44; ifi44l***	*Ifi44a1–a8; ifi44b; ifi44c1/2;* ***ifi44d****; ifi44e; ifi44f-1,-2,-4; -3, -5,-6 ; ifi44g*
IFIT	***ifit-1, -2, -3, -5;*** *ifit1b*	*ifita; ifitb1–4;* ***ifitc****;* ***ifitd1–3;*** *ifitd2*
LGAL	***lgals-9***, *-s9b,-s9c*	***lgals-9l1***, ***-s9l2****,-s9l3,-s9l4, s9l-5*
MS4A	***ms4a4a****; ms4a-2, -3, -5, -8, -12, -14, -15, -18*	*ms4a-a1; -a2; -a3; -a4 to -a7; -a8; -a9 to -a14; ms4a-b1 to b4; ms4a-c*
Mx	***mx1; mx2***	***mxa****,-b, -b2 to -d,* ***-e,*** *–f, -g, -h*
Conserved orthologous members in teleosts and tetrapods (old)		
CD9	***cd9***, *cd81, tspan2*	*cd9-a, -b,* ***cd9-c****, cd81-a, -b, tspan2-a, -b*
RLR	***ddx58/rigI; ifih1/mda5; dhx58/lgp2***	*ddx58/rigI; ifih1/mda5; dhx58/lgp2*
IRF	***irf-1, -2, -7, -9*** *irf3–6, -8*	*irf-1a,-**1b**,-2a,-2b,* ***-3?, -****4a,b,l, -5,- 6,* ***-7****, -8, -9, -10*
SOCS	***socs-1; socs-2****; socs-4 to -7; cish*	***socs1a****; socs1b; socs3a;* ***socs3b****; socs4; socs5a; socs-5b; socs6a; socs6b;* ***socs7****; socs8; cish*
STAT	***stat1; stat2****; stat3; stat4; stat5a; stat5b; stat6*	***stat1a****;* ***stat1b****; stat2; stat3; stat4; stat5.1; stat5.2; stat6*

[a]Only families with at least two ISGs were considered.
[b]ISGs are in bold (same criteria as for Fig. 7); fish genes not represented on the array are on gray background. Overall, the nomenclature was chosen to fit at best the phylogenetic relationships; similar names were not used for nonorthologs. Identity of zebrafish genes can be searched in Supplemental Table I.

whole larva, thus integrating the contribution of all tissues, either infected or put in contact with the secreted IFNs. The arbovirus CHIKV leads to a strong systemic IFN response in the zebrafish larva, and the genes with the strongest inductions could be immediately identified as a core set of canonical ISGs conserved in other fish, including in adult tissues, and in mammals. This set of IFN responsive genes was also induced, although more modestly, by the rhabdovirus IHNV in the zebrafish larva. In fact, rhabdoviruses can inhibit IFN responses through different mechanisms likely involving the P and NV proteins (38–43), and IHNV induces a relatively mild IFN response (44). This inhibition appears to play mostly upstream of IFN induction because recombinant IFN injection protects zebrafish from IHNV (26). Although ISGs are typically less strongly induced by IHNV compared with CHIKV, 16 features on the arrays were significantly induced by CHIKV but in fact repressed by IHNV, suggesting that antagonist pathways were implicated. Although the mechanisms of inhibition of IFN response by IHNV are beyond the scope of this study, our dataset might therefore provide clues about the genes involved.

In addition to highly induced orthologs of human ISGs, our analysis suggests that many ISGs common to fish and mammals can be induced at a more moderate level by CHIKV. For example, genes with an FC of 1.56–1.95 (with a p value of <0.05) were five times more frequent among zebrafish orthologs of human ISGs than they were for the whole gene set (Fig. 6). In fact, this observation suggests that 80% of the zebrafish orthologs of human ISGs within this FC interval are indeed truly upregulated by IFN. This provided us with a basis to estimate that the zebrafish possesses ~100 IFN-induced genes among its orthologs of human ISGs.

Apart from this core set of ISGs common to fish and humans, do we have evidence of lineage-specific gene families modulated by the viral infection? A striking feature of the CHIKV-induced responses of zebrafish larva was the lack of additional families of highly induced genes, compared with the human ISG set. Several large multigene families such as finTRIM and NLR are likely playing important roles in the fish (innate) immune responses because of their diversification patterns (45–47); strikingly, none of their members was found in our list of induced genes in the immature system of the zebrafish larva. There are, however, a few genes that are specifically induced in fish; for instance, the autophagy regulator *dram1* was strongly induced by CHIKV and found to be induced in an IFN-specific manner in trout (48), although it is not a typical ISG in humans. Alternatively, we identified four tetrapod specific genes families containing ISGs: *aim2/IF116*, *Apobec3*, *Clec4*, and *OAS*.

Additionally, noncoding RNAs, which are poorly conserved between species, constitute potentially important genes induced by viruses in a species-specific fashion. The trout gene *vig2* (restricted to salmonids) and the human *LINC00969* represent good examples of such ISGs (2, 49). In our microarray data, a few strongly induced probes apparently hybridized in regions encoding long coding transcripts, but we did not investigate this further.

Altogether, these observations suggest the presence of a shared core set of ISGs in fish and mammals, which we predict to contain at least 100 genes. Importantly, however, our study has been performed on larvae, and it is quite possibly that a larger set of ISGs may be found in adult zebrafish, in which the adaptive immune system is functional. This should be investigated in future studies.

How old is the core ISGs set?

ISGs follow several types of evolutionary patterns, and the analysis of families is particularly interesting in that respect. We observed that some families had diversified in the common ancestor of fish and tetrapods: as most human family members have a single ortholog (or a pair of paralogs due to the fish WGD) in zebrafish, this family had already diversified in the common ancestor to fishes and mammals. Such families, which we called "old," seem stabilized in both branches after the teleost/tetrapod split, with little evidence for lineage-specific diversification. Additionally, inducibility by IFN of the individual family members is also generally

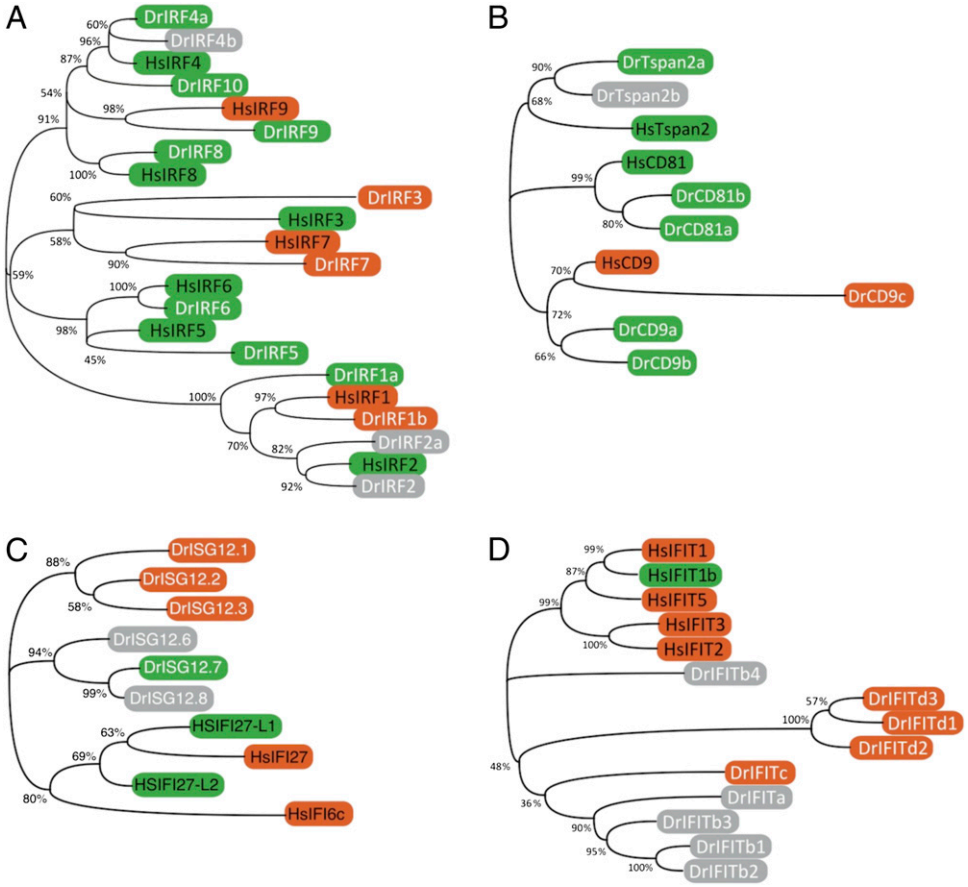

FIGURE 7. Different types of phylogenies of ISG-containing families. (**A** and **B**) Two examples of old families: IRF and CD9. (**C** and **D**) Two examples of new families: ISG12/IFI27 and IFIT. Background colors: orange for ISGs (see below), green for non-ISGs, gray if unknown. Human genes are shown with black letters; zebrafish genes are shown in white. Maximum likelihood trees with bootstrap values out of 1000 replicates are indicated. Human genes classified as ISGs according to their presence or absence on the list established by Schoggins et al. (2). Zebrafish genes were classified as ISGs when found induced >2.5-fold by CHIKV on our microrray dataset, with the exception of *irf3*, not present on the microarray but induced by IFN in fish as shown by Sun et al. (37) and verified by N.P. (unpublished data). ISG12.7 is on green background (non-ISG) but was slightly induced by CHIKV (FC = 1.88; $p < 1\%$). Accession numbers of sequences used: IRF: HsIRF1, NP_002189; HsIRF2, NP_002190; HsIRF3, NP_001562; HsIRF4, NP_002451; HsIRF5, NP_116032; HsIRF6, NP_006138; HsIRF7, NP_001563; HsIRF8, NP_002154; HsIRF9, NP_006075; DrIRF1, NP_001035442; DrIRF2, ENSDARP00000059229; DrIRF2A, B8JIT4; DrIRF3, NP_001137376; DrIRF4A, NP_001116182; DrIRF4B, XP_697730; DrIRF5, NP_998040; DrIRF6, NP_956892; DrIRF7, NP_956971; DrIRF8, NP_001002622; DrIRF9, NP_991273; DrIRF10, NP_998044; DrIRF11, NP_991310. CD9: HsCD9, NP_001760; HsCD81, NP_004347; HsTSPAN2, NP_005716; DrCD9a, NP_997784; DrCD9b, NP_998593; DrTSPAN2A, NP_001018160; DrCD81, NP_571593; DrCD81b, NP_001003735; DrCD9c, translation of GO937947; DrTSPAN2B, ENSDARP00000007110. ISG12/IFI27: HsIFI27, NP_001123552; HsIFI27L1, NP_660292; HsIFI27L2, NP_114425; HsIFI6, NP_075011; DrISG12.3, XP_704861; DrISG12.1, NP_001007133; DrISG12.2, NP_001007134; DrISG12.3, ENSDARG00000074217; DrISG12.4, ENSDARG00000078389; DrISG12.6, ENSDARG00000074754; DRISG12.7, ENSDARG00000075151; DrISG12.8, ENSDARG00000092895. IFIT: HsIFIT1, EAW50136; HsIFIT1B, NP_001010987; HsIFIT5, NP_036552; HsIFIT2, NP_001538; HsIFIT3, NP_001540; DrIFITb3, XP_695829; DrIFITb4, XP_695770; DrIFITb2, NP_001177393; DrIFITb1, NP_001177394; DrIFITa, XP_701096; DrIFITc, NP_001032654; DrIFITd3, XP_001334809; DrIFITd1, XP_001333807; DrIFITd2, XP_001334890. DrISG12.5 appeared to be partial and was not included.

conserved (Fig. 7, Table III). This pattern typically corresponds to regulatory components such as transcription factors or signal transduction proteins (e.g, IRFs, STATs, SOCS). As a result, the virus-responsive signaling machinery appears to be very well conserved between fish and mammals, with very similar feedback loops at play (Supplemental Table I). In contrast, we called "young" other families differentiated in parallel in each lineage from a single common ancestor gene. Those would be expected to evolve under high diversifying pressures, such as the ones dictated by the modalities of direct interactions with pathogens. This is indeed the case for such proteins belonging to the young MX or IFIT families (50). We can therefore predict that functionally uncharacterized ISGs from such young families, such as members of the ISG12/IFI27 or IFI44 families, should directly interact with some viral components.

Temporal and spatial regulation of ISGs

To complement the microarray study, performed at a single time point on extracts from entire larvae, we analyzed the kinetics (Fig. 2) and the spatial expression (Fig. 3) of a gene subset. All ISGs in this subset showed a very comparable kinetic that faithfully mirrored that of secreted *ifnφ1* induction. Remarkably, and despite it being widely accepted that all nucleated cells express type I IFN receptors, ISGs were expressed in a tissue-restricted pattern, with a prominent expression in the liver, the vasculature, and the gut, with minor gene-specific tissue preferences superimposed on this general pattern. Interestingly, this pattern matches partially the one of IFN-φ1 itself, with a strong expression in the liver (11). Such contrasted patterns were not expected, yet they are reminiscent of studies performed in mice with an MX/luciferase

reporter gene (51), where liver was observed to respond much more strongly than other organs to injected IFN or to Thogoto virus infection. Thus, strongly organ-biased expression of ISGs may well be the norm among vertebrates. It remains to be established whether this reflects local availability of IFNs or differential responsiveness of other organs.

Alternative pathways at play during IHNV infection

Whereas CHIKV infection induced a strong and protective IFN response, IHNV infection invariably leads to the death of the zebrafish larva. Many genes are induced by the INHV infection but poorly or not induced by CHIKV. Their upregulation is likely linked to the activation of IFN-independent pathways. This may be largely caused by extensive cell death due to viral cytopathic activity and subsequent inflammation.

Many mitochondrial genes were induced by IHNV, suggesting that this virus induces a general mitochondrial response potentially linked to apoptosis and oxidative reaction. Interestingly, a cellular oxidative response can suppress the IFN-α–induced assembly of STAT factors at the ISG promoters, thus potentially contributing to the knockdown of the IFN-induced response (52). Such an oxidative response may also be responsible for the induction of *mmp9* in epidermal cells that we observed by ISH, similar to what has been observed during bacterial infections (53).

A variety of ribosomal proteins are also modulated by IHNV, possibly in response to translational shut-off of host proteins achieved by rhabdoviruses. A downregulation of protein synthesis by IHNV infection have been reported before in rainbow trout (44).

Fkbp5 was strongly downregulated by the IHNV infection, although it is a mammalian ISG, and it is induced in chicken by the Newcastle disease virus (54). In fact, *fkbp5* is probably not an ISG in zebrafish, because it is not induced by CHIKV (nor, for that matter, is *fkbp4*, another possible ortholog of human *FKBP5*). FKBP5 links glucocorticoids to NF-κB signaling during viral infection (55), but its role in antiviral responses is still elusive. This immunophilin with peptidyl-prolyl-isomerase activity reminds one of cyclophilins, which are other targets of cyclosporine A and may be either deleterious or beneficial for virus infections (56). Whether FKBP5 downregulation has a positive or a negative impact on the response to IHNV remains to be determined.

Our study identified *ependymin*, a marker specific of brain perivascular cells, as a gene repressed by the IHNV, but not by CHIKV. The progressive reduction of expression during infection suggested that peripheral brain cells in which it was expressed might be targeted and killed by the virus. The WISH supported this notion, because the infected larvae lost completely *ependymin* expression in the dorsal cranium. Thus, transcriptome survey may lead not only to the identification of responding cells through localization of gene upregulation, but may also reveal virus cellular targets by extinction of specific markers.

In conclusion, our study characterizes the contrasted transcriptional responses of zebrafish to a fish rhabdovirus, IHNV, and a human arbovirus, CHIKV. The strong type I IFN response induced by CHIKV allowed us to greatly extend the list of zebrafish ISGs, many of which belong to multigene families. Their different evolutionary stories reflect their functional implication in antiviral pathways. Our transcriptome survey also led to the characterization of the spatial expression pattern of key up- or downregulated markers, providing an important reference set for the study of host–virus interactions in zebrafish, a powerful model where one can perform gene silencing, mutagenesis, or drug screening.

Acknowledgments

We thank Hannah Volkman for the *mmp9* probe and Abdenour Benmansour for helpful discussions.

Disclosures

The authors have no financial conflicts of interest.

References

1. Der, S. D., A. Zhou, B. R. Williams, and R. H. Silverman. 1998. Identification of genes differentially regulated by interferon α, β, or γ using oligonucleotide arrays. *Proc. Natl. Acad. Sci. USA* 95: 15623–15628.
2. Schoggins, J. W., S. J. Wilson, M. Panis, M. Y. Murphy, C. T. Jones, P. Bieniasz, and C. M. Rice. 2011. A diverse range of gene products are effectors of the type I interferon antiviral response. *Nature* 472: 481–485.
3. Sadler, A. J., and B. R. G. Williams. 2008. Interferon-inducible antiviral effectors. *Nat. Rev. Immunol.* 8: 559–568.
4. Schoggins, J. W., and C. M. Rice. 2011. Interferon-stimulated genes and their antiviral effector functions. *Curr. Opin. Virol.* 1: 519–525.
5. Brass, A. L., I.-C. Huang, Y. Benita, S. P. John, M. N. Krishnan, E. M. Feeley, B. J. Ryan, J. L. Weyer, L. van der Weyden, E. Fikrig, et al. 2009. The IFITM proteins mediate cellular resistance to influenza A H1N1 virus, West Nile virus, and dengue virus. *Cell* 139: 1243–1254.
6. Flajnik, M., and L. Du Pasquier. 2013. Evolution of the immune system. In *Fundamental Immunology*, 7th Ed. W. Paul, ed. Wolters Kluwer and Lippincott Willians & Wilkins, New York, p. 67–128.
7. Kanther, M., and J. F. Rawls. 2010. Host-microbe interactions in the developing zebrafish. *Curr. Opin. Immunol.* 22: 10–19.
8. Meijer, A. H., and H. P. Spaink. 2011. Host-pathogen interactions made transparent with the zebrafish model. *Curr. Drug Targets* 12: 1000–1017.
9. Tobin, D. M., F. J. Roca, S. F. Oh, R. McFarland, T. W. Vickery, J. P. Ray, D. C. Ko, Y. Zou, N. D. Bang, T. T. H. Chau, et al. 2012. Host genotype-specific therapies can optimize the inflammatory response to mycobacterial infections. *Cell* 148: 434–446.
10. Ludwig, M., N. Palha, C. Torhy, V. Briolat, E. Colucci-Guyon, M. Brémont, P. Herbomel, P. Boudinot, and J.-P. Levraud. 2011. Whole-body analysis of a viral infection: vascular endothelium is a primary target of infectious hematopoietic necrosis virus in zebrafish larvae. *PLoS Pathog.* 7: e1001269.
11. Palha, N., F. Guivel-Benhassine, V. Briolat, G. Lutfalla, M. Sourisseau, F. Ellett, C.-H. Wang, G. J. Lieschke, P. Herbomel, O. Schwartz, and J.-P. Levraud. 2013. Real-time whole-body visualization of Chikungunya virus infection and host interferon response in zebrafish. *PLoS Pathog.* 9: e1003619.
12. Herath, T. K., J. E. Bron, K. D. Thompson, J. B. Taggart, A. Adams, J. H. Ireland, and R. H. Richards. 2012. Transcriptomic analysis of the host response to early stage salmonid alphavirus (SAV-1) infection in Atlantic salmon *Salmo salar* L. *Fish Shellfish Immunol.* 32: 796–807.
13. Timmerhaus, G., A. Krasnov, P. Nilsen, M. Alarcon, S. Afanasyev, M. Rode, H. Takle, and S. M. Jørgensen. 2011. Transcriptome profiling of immune responses to cardiomyopathy syndrome (CMS) in Atlantic salmon. *BMC Genomics* 12: 459.
14. Huang, Y., X. Huang, Y. Yan, J. Cai, Z. Ouyang, H. Cui, P. Wang, and Q. Qin. 2011. Transcriptome analysis of orange-spotted grouper (*Epinephelus coioides*) spleen in response to Singapore grouper iridovirus. *BMC Genomics* 12: 556.
15. Lu, M.-W., F.-H. Ngou, Y.-M. Chao, Y.-S. Lai, N.-Y. Chen, F.-Y. Lee, and P. P. Chiou. 2012. Transcriptome characterization and gene expression of *Epinephelus* spp in endoplasmic reticulum stress-related pathway during betanodavirus infection in vitro. *BMC Genomics* 13: 651.
16. Krasnov, A., Ø. Kileng, S. Skugor, S. M. Jørgensen, S. Afanasyev, G. Timmerhaus, A.-I. Sommer, and I. Jensen. 2013. Genomic analysis of the host response to nervous necrosis virus in Atlantic cod (*Gadus morhua*) brain. *Mol. Immunol.* 54: 443–452.
17. Purcell, M. K., I. S. Marjara, W. Batts, G. Kurath, and J. D. Hansen. 2011. Transcriptome analysis of rainbow trout infected with high and low virulence strains of infectious hematopoietic necrosis virus. *Fish Shellfish Immunol.* 30: 84–93.
18. Martin, S. A. M., J. B. Taggart, P. Seear, J. E. Bron, R. Talbot, A. J. Teale, G. E. Sweeney, B. Høyheim, D. F. Houlihan, D. R. Tocher, et al. 2007. Interferon type I and type II responses in an Atlantic salmon (*Salmo salar*) SHK-1 cell line by the salmon TRAITS/SGP microarray. *Physiol. Genomics* 32: 33–44.
19. Stockhammer, O. W., A. Zakrzewska, Z. Hegedûs, H. P. Spaink, and A. H. Meijer. 2009. Transcriptome profiling and functional analyses of the zebrafish embryonic innate immune response to *Salmonella* infection. *J. Immunol.* 182: 5641–5653.
20. Levraud, J.-P., E. Colucci-Guyon, M. J. Redd, G. Lutfalla, and P. Herbomel. 2008. In vivo analysis of zebrafish innate immunity. *Methods Mol. Biol.* 415: 337–363.
21. Langmead, B., C. Trapnell, M. Pop, and S. L. Salzberg. 2009. Ultrafast and memory-efficient alignment of short DNA sequences to the human genome. *Genome Biol.* 10: R25.
22. van Soest, J. J., O. W. Stockhammer, A. Ordas, G. V. Bloemberg, H. P. Spaink, and A. H. Meijer. 2011. Comparison of static immersion and intravenous injection systems for exposure of zebrafish embryos to the natural pathogen *Edwardsiella tarda*. *BMC Immunol.* 12: 58.
23. Lutfalla, G., and G. Uze. 2006. Performing quantitative reverse-transcribed polymerase chain reaction experiments. *Methods Enzymol.* 410: 386–400.

24. Boudinot, P., L. M. van der Aa, L. Jouneau, L. Du Pasquier, P. Pontarotti, V. Briolat, A. Benmansour, and J.-P. Levraud. 2011. Origin and evolution of TRIM proteins: new insights from the complete TRIM repertoire of zebrafish and pufferfish. *PLoS ONE* 6: e22022.
25. Thisse, C., and B. Thisse. 2008. High-resolution in situ hybridization to whole-mount zebrafish embryos. *Nat. Protoc.* 3: 59–69.
26. Aggad, D., M. Mazel, P. Boudinot, K. E. Mogensen, O. J. Hamming, R. Hartmann, S. Kotenko, P. Herbomel, G. Lutfalla, and J.-P. Levraud. 2009. The two groups of zebrafish virus-induced interferons signal via distinct receptors with specific and shared chains. *J. Immunol.* 183: 3924–3931.
27. Tamura, K., D. Peterson, N. Peterson, G. Stecher, M. Nei, and S. Kumar. 2011. MEGA5: molecular evolutionary genetics analysis using maximum likelihood, evolutionary distance, and maximum parsimony methods. *Mol. Biol. Evol.* 28: 2731–2739.
28. Thisse, B., V. Heyer, A. Lux, V. Alunni, A. Degrave, I. Seiliez, J. Kirchner, J.-P. Parkhill, and C. Thisse. 2004. Spatial and temporal expression of the zebrafish genome by large-scale in situ hybridization screening. *Methods Cell Biol.* 77: 505–519.
29. Covassin, L., J. D. Amigo, K. Suzuki, V. Teplyuk, J. Straubhaar, and N. D. Lawson. 2006. Global analysis of hematopoietic and vascular endothelial gene expression by tissue specific microarray profiling in zebrafish. *Dev. Biol.* 299: 551–562.
30. Biacchesi, S., M. LeBerre, A. Lamoureux, Y. Louise, E. Lauret, P. Boudinot, and M. Brémont. 2009. Mitochondrial antiviral signaling protein plays a major role in induction of the fish innate immune response against RNA and DNA viruses. *J. Virol.* 83: 7815–7827.
31. Lauksund, S., T. Svingerud, V. Bergan, and B. Robertsen. 2009. Atlantic salmon IPS-1 mediates induction of IFNa1 and activation of NF-κB and localizes to mitochondria. *Dev. Comp. Immunol.* 33: 1196–1204.
32. Levraud, J.-P., P. Boudinot, I. Colin, A. Benmansour, N. Peyrieras, P. Herbomel, and G. Lutfalla. 2007. Identification of the zebrafish IFN receptor: implications for the origin of the vertebrate IFN system. *J. Immunol.* 178: 4385–4394.
33. Langevin, C., E. Aleksejeva, G. Passoni, N. Palha, J.-P. Levraud, and P. Boudinot. 2013. The antiviral innate immune response in fish: evolution and conservation of the IFN system. *J. Mol. Biol.* 425: 4904–4920.
34. Lyles, D. S. 2000. Cytopathogenesis and inhibition of host gene expression by RNA viruses. *Microbiol. Mol. Biol. Rev.* 64: 709–724.
35. Howe, K., M. D. Clark, C. F. Torroja, J. Torrance, C. Berthelot, M. Muffato, J. E. Collins, S. Humphray, K. McLaren, L. Matthews, et al. 2013. The zebrafish reference genome sequence and its relationship to the human genome. *Nature* 496: 498–503.
36. Moffatt, P., M.-H. Gaumond, P. Salois, K. Sellin, M.-C. Bessette, E. Godin, P. T. de Oliveira, G. J. Atkins, A. Nanci, and G. Thomas. 2008. Bril: a novel bone-specific modulator of mineralization. *J. Bone Miner. Res.* 23: 1497–1508.
37. Sun, B., B. Robertsen, Z. Wang, and B. Liu. 2009. Identification of an Atlantic salmon IFN multigene cluster encoding three IFN subtypes with very different expression properties. *Dev. Comp. Immunol.* 33: 547–558.
38. Thoulouze, M. I., E. Bouguyon, C. Carpentier, and M. Brémont. 2004. Essential role of the NV protein of *Novirhabdovirus* for pathogenicity in rainbow trout. *J. Virol.* 78: 4098–4107.
39. Vidy, A., M. Chelbi-Alix, and D. Blondel. 2005. Rabies virus P protein interacts with STAT1 and inhibits interferon signal transduction pathways. *J. Virol.* 79: 14411–14420.
40. Brzózka, K., S. Finke, and K.-K. Conzelmann. 2006. Inhibition of interferon signaling by rabies virus phosphoprotein P: activation-dependent binding of STAT1 and STAT2. *J. Virol.* 80: 2675–2683.
41. Chelbi-Alix, M. K., A. Vidy, J. El Bougrini, and D. Blondel. 2006. Rabies viral mechanisms to escape the IFN system: the viral protein P interferes with IRF-3, Stat1, and PML nuclear bodies. *J. Interferon Cytokine Res.* 26: 271–280.
42. Choi, M. K., C. H. Moon, M. S. Ko, U. H. Lee, W. J. Cho, S. J. Cha, J. W. Do, G. J. Heo, S. G. Jeong, Y. S. Hahm, et al. 2011. A nuclear localization of the infectious haematopoietic necrosis virus NV protein is necessary for optimal viral growth. *PLoS ONE* 6: e22362.
43. Kim, M. S., and K. H. Kim. 2013. The role of viral hemorrhagic septicemia virus (VHSV) NV gene in TNF-α- and VHSV infection-mediated NF-κB activation. *Fish Shellfish Immunol.* 34: 1315–1319.
44. MacKenzie, S., J. C. Balasch, B. Novoa, L. Ribas, N. Roher, A. Krasnov, and A. Figueras. 2008. Comparative analysis of the acute response of the trout, *O. mykiss*, head kidney to in vivo challenge with virulent and attenuated infectious hematopoietic necrosis virus and LPS-induced inflammation. *BMC Genomics* 9: 141.
45. Laing, K. J., M. K. Purcell, J. R. Winton, and J. D. Hansen. 2008. A genomic view of the NOD-like receptor family in teleost fish: identification of a novel NLR subfamily in zebrafish. *BMC Evol. Biol.* 8: 42.
46. Stein, C., M. Caccamo, G. Laird, and M. Leptin. 2007. Conservation and divergence of gene families encoding components of innate immune response systems in zebrafish. *Genome Biol.* 8: R251.
47. van der Aa, L. M., J.-P. Levraud, M. Yahmi, E. Lauret, V. Briolat, P. Herbomel, A. Benmansour, and P. Boudinot. 2009. A large new subset of TRIM genes highly diversified by duplication and positive selection in teleost fish. *BMC Biol.* 7: 7.
48. O'Farrell, C., N. Vaghefi, M. Cantonnet, B. Buteau, P. Boudinot, and A. Benmansour. 2002. Survey of transcript expression in rainbow trout leukocytes reveals a major contribution of interferon-responsive genes in the early response to a rhabdovirus infection. *J. Virol.* 76: 8040–8049.
49. Boudinot, P., S. Salhi, M. Blanco, and A. Benmansour. 2001. Viral haemorrhagic septicaemia virus induces *vig-2*, a new interferon-responsive gene in rainbow trout. *Fish Shellfish Immunol.* 11: 383–397.
50. Kochs, G., and O. Haller. 1999. GTP-bound human MxA protein interacts with the nucleocapsids of Thogoto virus (Orthomyxoviridae). *J. Biol. Chem.* 274: 4370–4376.
51. Pulverer, J. E., U. Rand, S. Lienenklaus, D. Kugel, N. Zietara, G. Kochs, R. Naumann, S. Weiss, P. Staeheli, H. Hauser, and M. Köster. 2010. Temporal and spatial resolution of type I and III interferon responses in vivo. *J. Virol.* 84: 8626–8638.
52. Di Bona, D., M. Cippitelli, C. Fionda, C. Cammà, A. Licata, A. Santoni, and A. Craxì. 2006. Oxidative stress inhibits IFN-α-induced antiviral gene expression by blocking the JAK-STAT pathway. *J. Hepatol.* 45: 271–279.
53. Hall, C. J., R. H. Boyle, J. W. Astin, M. V. Flores, S. H. Oehlers, L. E. Sanderson, F. Ellett, G. J. Lieschke, K. E. Crosier, and P. S. Crosier. 2013. Immunoresponsive gene 1 augments bactericidal activity of macrophage-lineage cells by regulating β-oxidation-dependent mitochondrial ROS production. *Cell Metab.* 18: 265–278.
54. Park, M.-S., J. Steel, A. García-Sastre, D. Swayne, and P. Palese. 2006. Engineered viral vaccine constructs with dual specificity: avian influenza and Newcastle disease. *Proc. Natl. Acad. Sci. USA* 103: 8203–8208.
55. Karin, M., and Y. Ben-Neriah. 2000. Phosphorylation meets ubiquitination: the control of NF-κB activity. *Annu. Rev. Immunol.* 18: 621–663.
56. He, H., D. Zhou, W. Fan, X. Fu, J. Zhang, Z. Shen, J. Li, J. Li, and Y. Wu. 2012. Cyclophilin A inhibits rotavirus replication by facilitating host IFN-I production. *Biochem. Biophys. Res. Commun.* 422: 664–669.